Received: 26 September 2020 | Revised: 26 October 2020 | Accepted: 28 October 2020

DOI: 10.1002/pol.20200673

RESEARCH ARTICLE

JOURNAL OF POLYMER SCIENCE WILEY

Polymorphism of a semi-crystalline diketopyrrolopyrrole-terthiophene polymer

Mengmeng Li[1,2,3,4] | **Pieter J. Leenaers**[2] | **Junyu Li**[2] | **Martijn M. Wienk**[2] | **René A. J. Janssen**[2,3]

[1]Key Laboratory of Microelectronic Devices and Integrated Technology, Institute of Microelectronics, Chinese Academy of Sciences, Beijing, China

[2]Molecular Materials and Nanosystems, Institute for Complex Molecular Systems, Eindhoven University of Technology, Eindhoven, The Netherlands

[3]Dutch Institute For Fundamental Energy Research, Eindhoven, The Netherlands

[4]School of Electronic, Electrical and Communication Engineering, University of Chinese Academy of Sciences, Beijing, China

Correspondence
Mengmeng Li, Key Laboratory of Microelectronic Devices and Integrated Technology, Institute of Microelectronics, Chinese Academy of Sciences, Beijing 100029, China.
Email: limengmeng@ime.ac.cn

René A. J. Janssen, Eindhoven University of Technology, P.O. Box 513, 5600 MB Eindhoven, The Netherlands.
Email: r.a.j.janssen@tue.nl

Funding information
FP7 Ideas: European Research Council, Grant/Award Number: 339031; Ministerie van Onderwijs, Cultuur en Wetenschap, Grant/Award Number: 024.001.035; National Key R&D Program of China, Grant/Award Number: 2019YFA0706100; Nederlandse Organisatie voor Wetenschappelijk Onderzoek; National Natural Science Foundation of China, Grant/Award Number: 62074163

Abstract

Few semiconducting polymers are known that possess more than one semi-crystalline structure. Guidelines for rationalizing or creating polymorphism in these materials do not exist. Two different semi-crystalline polymorphs, β_1 and β_2, and an amorphous α phase have recently been identified for alternating diketopyrrolopyrrole-quaterthiophene copolymers (PDPP4T). The polymorphs differ structurally by the π–π stacking distance, and electronically by the optical bandgap and charge carrier mobility. Here we investigate the corresponding terthiophene (PDPP3T) derivatives, to study the effect of the relative orientation of adjacent DPP units on the polymorphism. In PDPP3T, the relative orientation of DPP units alternates along the chain, while in PDPP4T it is constant. We show that the two polymorphs, β_1 and β_2, can also be generated for a PDPP3T polymer in solution and thin film. Interestingly, compared to PDPP4T, more solvents can induce the two distinct semi-crystalline polymorphs for PDPP3T via a $\beta_1 \rightarrow \alpha \rightarrow \beta_2$ polymorphic transition.

KEYWORDS

aggregation, chain orientation, diketopyrrolopyrrole polymers, electronic devices, polymorphism

1 | INTRODUCTION

Semiconducting polymers have attracted extensive attention for application in flexible, low cost, solution-processable electronic devices, including organic light-emitting diodes (OLEDs), organic field-effect transistors (OFETs), and organic solar cells (OSCs).[1–5] Many conjugated polymers used in OFETs and OSCs are semi-crystalline and consist of a mixture of spaghetti-like amorphous domains and relatively ordered crystalline regions that exert a critical impact on their device performance.[6] Substantial effort has been invested to study and control the extent of crystallinity via the solution temperature, solvent quality, chemical structure, molecular weight and pre- or post-treatments. An order to disorder mechanism describes the transition between crystalline and amorphous phases.[7,8] In few cases, polymorphs have been identified in which two distinctly different semi-crystalline phases (β_1 and β_2) exist next to the amorphous (α) phase. Examples include poly(3-hexylthiophene) (P3HT), poly[[*N*,*N*′-bis(2-octyldodecyl)-naphthalene-1,4,5,8-bis(dicarboximide)-2,6-diyl]-alt-5,5′-(2,2′-bithiophene)] P(NDI2OD-T2), and poly[2,6-(4,4-bis-(2-ethylhexyl)-4H-cyclopenta[2,1-*b*;3,4-*b*′]dithiophene)-alt-4,7(2,1,3-benzothiadiazole)] (PCPDTBT).[9–13]

By controlling the nature of solvent, we recently showed that it also is possible to generate two distinctly different semi-crystalline polymorphs (β_1 and β_2) in narrow-bandgap alternating diketopyrrolopyrrole-quaterthiophene (PDPP4T) polymers (Figure 1).[14,15] Polymers with diketopyrrolopyrrole (DPP) units attract considerable attention for application in organic field-effect transistors and organic solar cells for which their semi-crystalline structure and three-dimensional packing are important to control.[16–24] This is also evident from the two polymorphs PDPP4T which differ structurally by the π–π stacking distance, and electronically by the optical bandgap and charge carrier mobility.[14,15] The main structural difference between the two polymorphs inferred from two-dimensional grazing-incidence wide-angle X-ray scattering (2D-GIWAXS) is the closer π–π stacking distance, while the lamellar spacing remains virtually the same. Linear alkyl chains on the DPP unit seem key to form the β_2 polymorph for PDPP4T polymers. By varying the length of linear alkyl chains on the DPP units, we found that a $\beta_1 \rightarrow \alpha \rightarrow \beta_2$ polymorphic transition proceeds readily for alkyl side chains of intermediate length (i.e., nonyl and dodecyl), but that for either short or long (i.e., hexyl or pentadecyl) side chains it is more difficult to generate the β_1 or β_2 polymorph, respectively, due to too low or too high solubility.[15]

To learn more about the structural molecular parameters that induce or influence polymorphism in PDPP*n*T polymers, we here investigate the corresponding PDPP3T polymer with a terthiophene (3T) conjugated segment in the main chain instead of 4T (Figure 1). Assuming that adjacent thiophenes adopt an s-*trans* conformation,[25,26] the relative orientation of the DPP units along the main chain then changes from parallel in PDPP4T to an alternating (right–left) orientation in PDPP3T as a consequence of the odd number of thiophene rings in the repeat unit of PDPP3T (Figure 2). This then leads to alternating large and small separations between the linear alkyl chains and at the same time the branched alkyl chains no longer have an *anti* orientation,[17] but would be present in *syn* oriented pairs. We note that for a PDPP3F polymer with long linear (tetradecyl) side chains on the DPP units and terfuran (3F) conjugated segments, scanning tunneling microscopy has shown that on an Au(111) surface the tendency to maximize alkyl chain interactions, results in a conformational twist that causes one of the furan-furan linkages to be s-*cis*. This then restores the parallel orientation of the tetradecyl chains.[27] In both cases, one may expect an influence on the polymorphism, because the main chain packing will be affected by the structural packing of the adjacent alkyl chains and/or conformational changes in the backbone.

Because of the lower number of thiophene rings per repeat unit in PDPP3T than in PDPP4T we reasoned that reducing the length of the alkyl chains compared to R-PDPP4T-HD (with R = nonyl or decyl, Figure 1) would be necessary to achieve a good balance between solubility and tendency to aggregate and crystallize. Hence, we prepared two versions of PDPP3T, one with a relative short hexyl chain on DPP and the branched 2′-hexyldecyl chains on the adjacent thiophenes (H-PDPP3T-HD) and one with a long dodecyl chain on DPP, but shorter

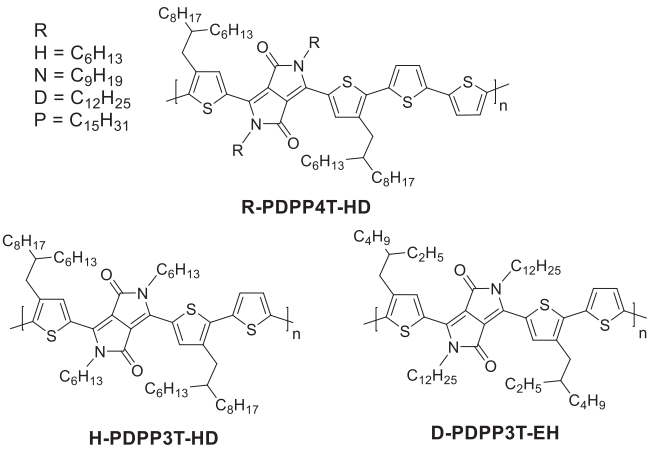

FIGURE 1 Chemical structures of the PDPP4T and PDPP3T polymers with linear alkyl chains (H, N, D, P) on the DPP unit and the branched alkyl chains (EH or HD) on the thiophene rings adjacent to the DPP

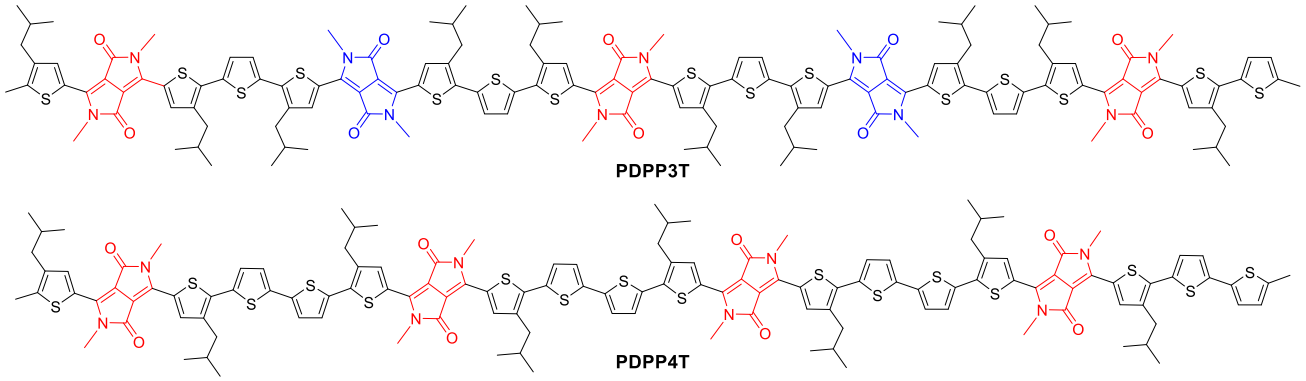

FIGURE 2 Schematic of the relative orientation of the DPP units in PDPP3T (right/left) and PDPP4T (parallel) [Color figure can be viewed at wileyonlinelibrary.com]

2′-ethylhexyl chains on thiophene (D-PDPP3T-EH) (Figure 1). Here, we demonstrate that for H-PDPP3T-HD the amorphous α-phase predominates, but that for D-PDPP3T-EH the solubility/aggregation balance is restored such that β_1 and β_2 can both be formed in chloroform (CF)—1,2,4-trichlorobenzene (TCB) mixtures and films cast thereof. The closer π–π stacking distance in the β_2 phase facilitates charge transport, doubling the field-effect mobility. The redshifted absorption of the β_2 phase noticeably contributes to the external quantum efficiency (EQE) in solar cells. It is also found that more solvents, including chlorobenzene (CB) and 1,2-dichlorobenzene (DCB), can generate β_2 polymorph for D-PDPP3T-EH compared to PDPP4Ts.

2 | EXPERIMENTAL

2.1 | Materials

The polymers were synthesized according to the literature.[28] By measuring gel permeation chromatography (GPC) in DCB at 140°C on a PL-GPC 120 system with a PL-GEL 10 mm MIXED-C column as the eluent and polystyrene as internal standards, the molecular weight (M_n) and polydispersity index (PDI) are 23.0 kg/mol and 2.13 for H-PDPP3T-HD, and 39.0 kg/mol and 2.31 for D-PDPP3T-EH.

2.2 | Characterization

A PerkinElmer Lambda 1050 spectrophotometer was used to measure UV–vis–NIR absorption for solution and thin films, and an Edinburgh Instruments FLSP920 double-monochromator luminescence spectrometer, equipped with a nitrogen-cooled near-IR sensitive photomultiplier (Hamamatsu), was utilized to record corresponding photoluminescence. 2D-GIWAXS was performed based on a Xenocs-SAXS/WAXS system, where the X-ray wavelength was 1.5418 Å and the fixed angle was 0.2° for X-ray irradiation. Before measurement, the thin films spin-coated from various solutions were annealed at 100°C for 30 min to remove residual solvent.

2.3 | Device fabrication and electrical characterization

Transistors with a bottom-contact top-gate architecture were fabricated, in which the source and drain electrodes with 50 nm in thickness (the ratio of channel length to width is 1/20) were deposited by Au evaporation. A CYTOP insulator was spin coated on top of polymer thin films as dielectric layer followed by annealing at 100°C for 1 hr, and finally 50-nm Ag was evaporated as gate electrode. A Keithley 4200-SCS was used for all standard OFET measurement under vacuum.

3 | RESULTS AND DISCUSSION

The optical absorption of H-PDPP3T-HD in CF shows a structureless band that maximizes at 668 nm (Figure 3a). The absence of any fine structure strongly suggests that the polymer is in a molecular dissolved, amorphous α phase. In TCB, the absorption redshifts to 690 nm, but with no clear sign of aggregation. The result that H-PDPP3T-HD is almost molecularly dissolved can be attributed to the two 2′-hexyldecyl chains that enhance the solubility.

Figure 3b shows the UV–vis–NIR absorption spectra of D-PDPP3T-EH in CF:TCB mixtures. When dissolved in pure CF (1:0), the first (0–0) and second (0–1) vibronic

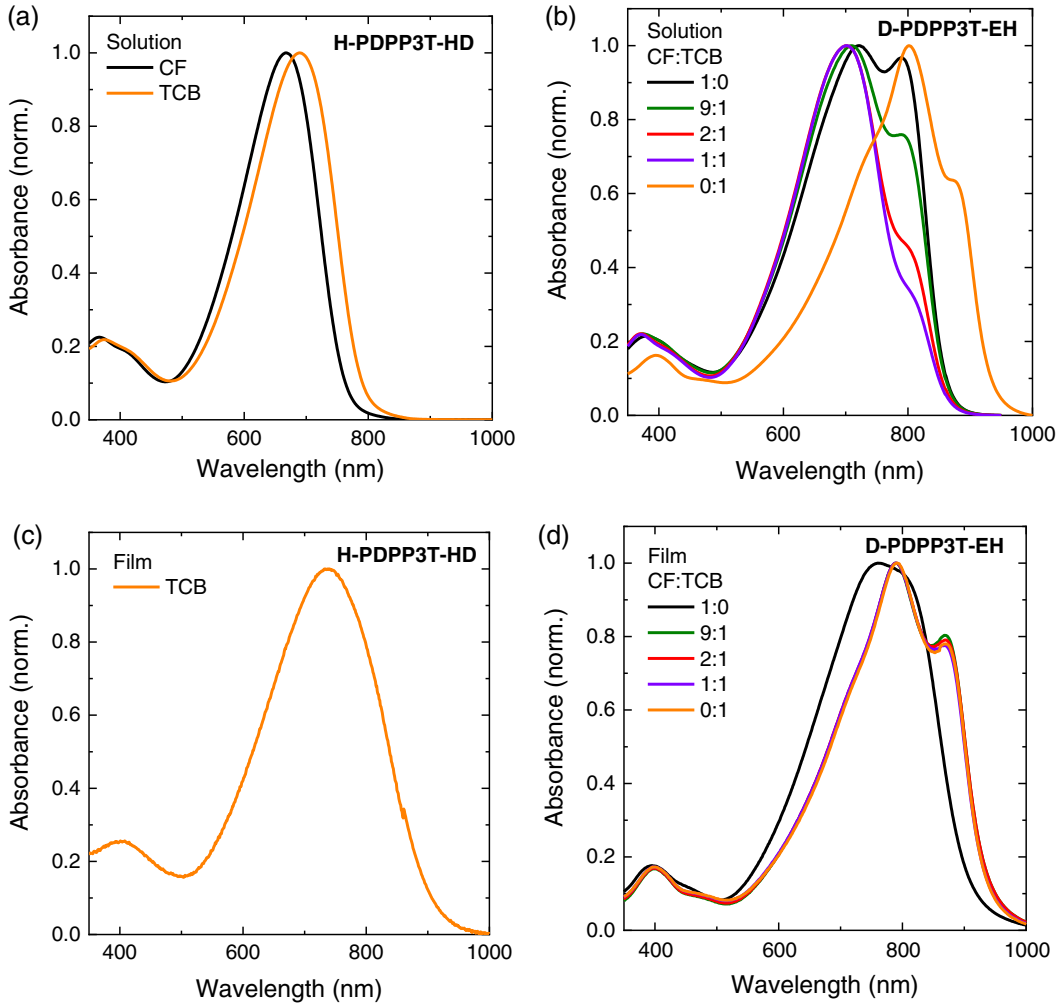

FIGURE 3 UV–vis–NIR absorption spectra. (a) H-PDPP3T-HD in CF and TCB. (b) D-PDPP3T-EH in CF:TCB (v/v) mixtures. The polymer concentration is around 0.4 μM (calculated fromM_n). (c) H-PDPP3T-HD film cast from TCB. (d) D-PDPP3T-EH films cast from CF:TCB mixtures. Thin films were spin coated from solutions with a polymer concentration of 3 mg/mL [Color figure can be viewed at wileyonlinelibrary.com]

bands of an aggregated β_1 phase are observed at 789 and 720 nm. In CF:TCB mixtures, the intensity of the 0–0 absorption peak decreases with an increasing amount of TCB and the spectrum starts to resemble that of H-PDPP3T-HD in Figure 3a. We attribute this to a transition from β_1 to α. In pure TCB (0:1), the spectrum of D-PDPP3T-EH shows a considerable redshift, with a new absorption maximum at 803 nm and a shoulder at 872 nm (Figure 3b). This shift and the high-wavelength shoulder are characteristic for the formation of the β_2 phase.[14,15] Hence, absorption spectroscopy reveals the generation of the β_2 polymorph in solution containing TCB.

H-PDPP3T-HD shows a broad structureless absorption in thin films, of which the onset and peak maximum redshifted considerably compared to the spectrum of the solution (Figure 3c). D-PDPP3T-EH films deposited from pure CF (1:0) show no evidence of a β_2 phase (Figure 3d), but when TCB is present in the casting solution a distinct new absorption peak at 868 nm emerges in the spectrum of the film. Figure 3d reveals that β_2 formation in films is virtually independent of the TCB content in the casting solution between 10 and 100%. This originates from the large differences in boiling point (214 vs. 61°C) and vapor pressure (0.46 vs. 197 mm Hg at 25°C) between TCB and CF, which causes that in the final stages of film formation only TCB remains, irrespective of the initial CF:TCB ratio.[14,15]

The polymorphism established for D-PDPP3T-EH also influences the fluorescence spectra. Figure 4a shows that photoluminescence of the β_1 phase of D-PDPP3T-EH in CF solution, recorded with excitation at 750 nm, maximizes at 865 nm. From the absorption spectra we inferred that at CF:TCB ratio of 1:1 most β_1 phase has transformed to the α phase (Figure 3b). As a result, also

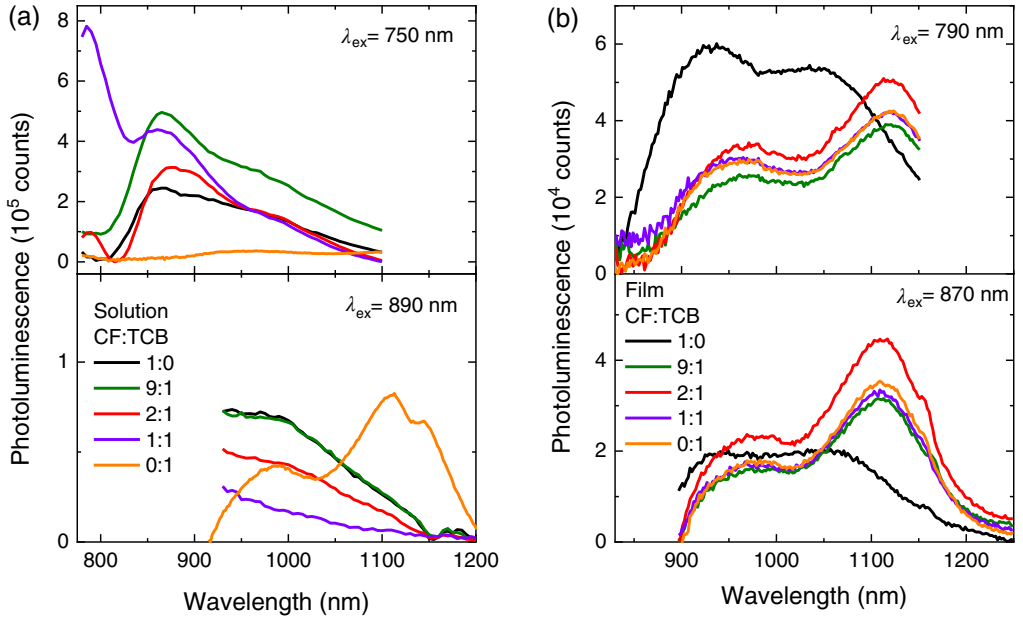

FIGURE 4 Photoluminescence spectra. (a) D-PDPP3T-EH dissolved in CF:TCB mixtures. (b) D-PDPP3T-EH thin films fabricated from CF:TCB mixtures. Thin films were spin coated from solutions with a polymer concentration of 3 mg/mL [Color figure can be viewed at wileyonlinelibrary.com]

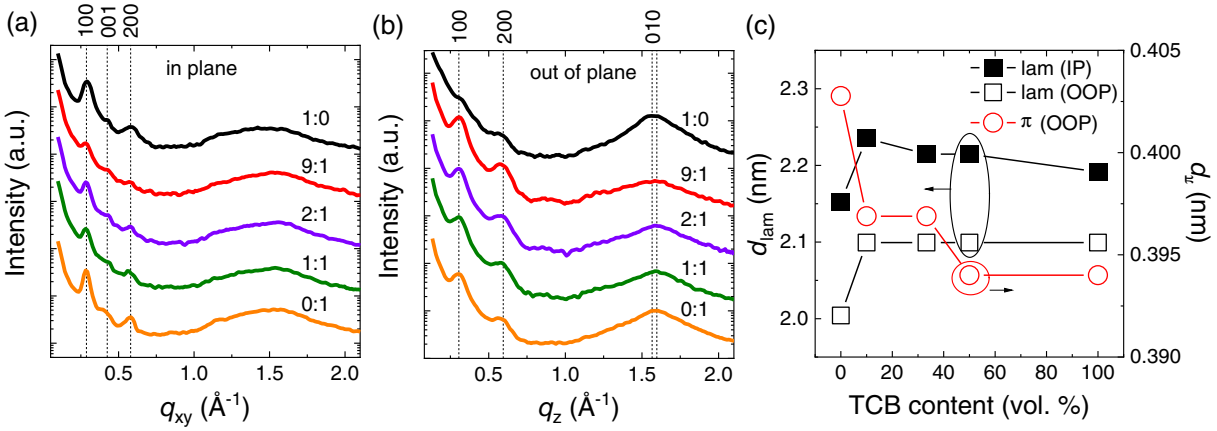

FIGURE 5 (a) 2D-GIWAXS in-plane profiles of D-PDPP3T-EH thin films spin coated from CF:TCB mixtures. (b) Corresponding out-of-plane profiles. (c) Lamellar spacing (d_{lam}) and π-stacking distance (d_π) as a function of TCB content. The vertical dashed lines in panels (a) and (b) are drawn to enable comparison of the vertically stacked GIWAXS profiles [Color figure can be viewed at wileyonlinelibrary.com]

the photoluminescence of D-PDPP3T-EH shifts to 785 nm in the 1:1 CF:TCB mixture. This confirms the $\beta_1 \rightarrow \alpha$ transition when the CF solution becomes richer in TCB. In pure TCB, the emission of D-PDPP3T-EH is negligible when excited at 750 nm, but when excitation wavelength is shifted to 890 nm, that is, at the characteristic peak of the β_2 phase, new emission peaks at 990 and 1110 nm appear (Figure 4a). This is the emission of the β_2 phase. In the photoluminescence spectra of thin films, the effect of the polymorphism is also evident. The photoluminescence of films cast from pure CF peaks at 930 and 1040 nm for β_1, but when TCB is present in the casting solution, the peaks shift to 970 and 1110 nm for β_2 (Figure 4b). The fluorescence of the films is not strongly dependent on the excitation wavelength used, 790 or 870 nm.

Microstructures of the β_1 and β_2 polymorphs of D-PDPP3T-EH were characterized by 2D-GIWAXS (Figure S1). Resultant in-plane and out-of-plane profiles are shown in Figure 5. All thin films were annealed at 100°C for 30 min. Under nitrogen atmosphere to remove residual solvents. In the in-plane profiles, the (100) and

(200) reflections are visible for all samples, characteristic of the lamellar arrangement of polymer backbones with a distance (d_{lam}) of 2.1 to 2.2 nm (Figure 5a). In between the (100) and (200) reflections a reflection is observed that possibly corresponds to the spacing along the polymer backbone direction (001) (1.46 nm), although the expected length of the repeat unit is somewhat larger (~1.65 nm). Clear (100) and (200) scattering peaks of the lamellar stacking are present for all films in the out-of-plane profiles (Figure 5b) next to a (010) diffraction peak that is attributed to π–π stacking and that is overlapping with an amorphous peak. The position of the (010) peak depends on the solvent mixture used to cast the films and shifts to slightly higher q values as the TCB contents increases (Figure 5b). Quantitative analysis was conducted to estimate d_{lam} and π-stacking distance (d_π) (Figure 5c). It is clear that d_{lam} of β_2 films made from solutions containing TCB (9:1, 2:1, 1:1, and 0:1) are slightly larger than that of the β_1 sample made from pure CF (1:0) in both in-plane and out-of-plane directions. Furthermore, β_2 possesses a smaller d_π than β_1, indicating a closer packing. The closer π–π stacking of β_2 is consistent with its redshifted absorption compared to β_1 (Figure 3d). The difference in lattice parameters observed for the β_1 and β_2 polymorphs of D-PDPP3T-EH are consistent with our previous study on PDPP4T polymers.[14,15]

It is further intriguing that d_{lam} = 2.1–2.2 nm for D-PDPP3T-EH is close to the values of d_{lam} = 2.1 and 2.3 nm found for N-PDPP4T-HD and D-PDPP4T-HD, while those of H-PDPP4T-HD (1.9 nm) and P-PDPP4T-HD (2.5 nm) are much shorter or much larger, respectively.[15] It thus appears that the PDPPnT polymers that have d_{lam} close to 2.2 nm readily provide the $\beta_1 \rightarrow \alpha \rightarrow \beta_2$ polymorphic transition in solution, while those with a shorter or longer d_{lam} have too low or too high solubility.[15] For constant d_π, d_{lam} gauges the amount of side chain per unit length of main chain and hence for semi-crystalline PDPPnT polymers d_{lam} is related to solubility.

Besides the difference in d_π, the reflection intensity of the (100) peak of D-PDPP3T-EH in the out-of-plane profiles is much weaker when cast from pure CF (1:0) than for films cast with TCB. This implies a difference in the orientational distribution for β_1 and β_2 polymorphs, despite their predominant face-on arrangement. To quantify the proportion of face-on orientation, the intensity of (100) peak was plotted as pole figure for the azimuthal angle between −90° and 90°. Figure S2 reveals that the β_1 polymorph exhibits more (71%) face-on population than β_2 (34–55%).

It is generally believed that a small d_π can reduce the energy barrier for interchain charge hopping, facilitating charge transport.[29] To elucidate the influence of polymorphism on charge transport, polymer field-effect transistors were fabricated with the top-gate bottom-contact architecture. Before the deposition of D-PDPP3T-EH layer, Au electrodes (source and drain) were functionalized with a 2,3,4,5,6-pentafluorothiophenol self-assembled monolayer. A CYTOP insulator layer was spin coated as dielectric on top of the D-PDPP3T-EH layers. The β_1 polymorph was generated from pure CF (1:0) and β_2 from a 2:1 CF:TCB mixture. The transfer and output characteristics (Figure 6a,b) of the transistors show for both polymorphs the typical linear/saturation behavior for hole transport. At the drain voltage (V_{DS}) of −30 V, the drain current ($-I_{DS}$) for the β_2 polymorph (2:1) is always higher than that of β_1 (1:0) when increasing the gate voltage (V_{GS}) from −0.6 to −30 V. The saturated field-effect mobility (μ_h) that is extracted from the transfer curve is 0.27 ± 0.02 cm^2 V^{-1} s^{-1} for β_2, almost doubled compared to β_1 (0.15 ± 0.02 cm^2 V^{-1} s^{-1}). This

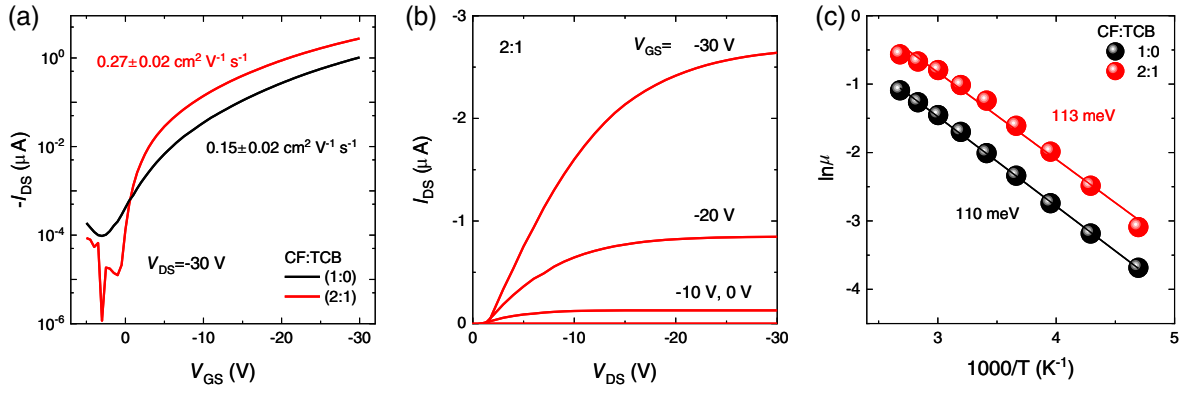

FIGURE 6 (a) Transfer characteristics of D-PDPP3T-EH field-effect transistors fabricated from 1:0 (β_1) and 2:1 (β_2) CF:TCB solutions. A drain voltage (V_{DS}) of −30 V is applied. (b) Corresponding output characteristics. (c) Temperature dependent field-effect mobility and corresponding activation energies forβ_1(1:0) andβ_2(2:1) polymorphs [Color figure can be viewed at wileyonlinelibrary.com]

enhanced mobility is attributed to the closer polymer packing of β_2. The improvement of transistor performance in the presence of β_2 is further supported by the increased on/off ratio (I_{on}/I_{off}) and decreased threshold voltage (V_T), as summarized in Table 1. The activation energy (E_A) estimated from temperature dependent transistor measurement is almost independent of polymorphism, as shown in Figure 6c.

Bulk-heterojunction solar cells with D-PDPP3T-EH as donor and [70]PCBM as acceptor material were fabricated from CF and from a 94:6 CF:TCB mixture. Details can be found in the Supporting Information (Table S1 and Figure S3). When the blend layer is cast from CF, D-PDPP3T-EH is present in the β_1 polymorph, but with 6% TCB the β_2 phase is formed as evidenced by significant (49%) external quantum efficiency at the characteristic wavelength (870 nm) of the β_2 phase.

For PDPP4T-HD polymers, we found that next to TCB also 1,1,2,2-tetrachloroethane (TCE) is able to induce the growth of the β_2 polymorph.[14,15] On the other hand, DCB and 1-chloronaphthalene were unable to induce β_2 for the PDPP4T-HD polymers.[14] Figure 7 reveals that for D-PDPP3T-EH several chlorinated solvents can induce the β_2 polymorph after aging. When aging a TCE solution of D-PDPP3T-EH, the characteristic peak of β_2 at 879 nm becomes stronger, and the absorption at 688 nm of the α phase clearly decreases, consistent with an $\alpha \rightarrow \beta_2$ polymorphic transition. CB and DCB are also able to form the β_2 polymorph. Although the absorbance at 879 nm is still weak after aging for 3 hr, a noticeable and distinguishable absorption peak is observed after 21 hr for both CB and DCB, indicative of β_2 formation.

Although it is an intriguing question, it is presently not clear why certain solvents favor either β_1 or β_2 phase. Our previous study on R-PDDP4T-HD polymers (Figure 1) demonstrated that formation of polymorphs β_1 or β_2 in CF:TCB mixtures is controlled by the alkyl side chains and the solubility that arises from it.[15] Shorter side chains (R = H, lower solubility) favor β_2 and longer side chains (R = P, higher solubility) give mainly β_1. At intermediate lengths (R = N and D) both phases can form. Hence, to have both β_1 and β_2 the solubility should be balanced. This also appears for D-PDPP3T-EH where the $\beta_1 \rightarrow \alpha \rightarrow \beta_2$ transition can be induced by gradually replacing CF by TCB (Figure 3b). For D-PDPP3T-EH the β_2 phase is seen in several halogenated solvents (Figure 4) while for D-PDDP4T-HD β_2 phase formation only occurs TCB and TCE.[14] So far, we have not been able to make a correlation between formation of β_1 or β_2 and the nature of the solvent. Comparison with Hansen dispersion, polar, and hydrogen bonding solubility parameters for polymers does not give a clear distinction (Table S2).

TABLE 1 Impact of polymorphism on transistor characteristics

	μ_h ($cm^2\ V^{-1}\ s^{-1}$)	V_T (V)	I_{on}/I_{off}	E_A (meV)
β_1	0.15 ± 0.02	−11 ± 1	10^4	110
β_2	0.27 ± 0.02	−7 ± 1	10^6	113

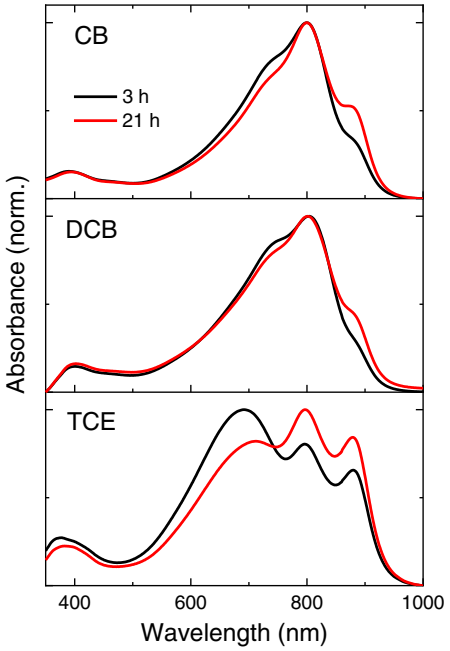

FIGURE 7 Polymorphism of D-PDPP3T-EH in CB, DCB, and TCE solutions. Solutions are aged at room temperature for 3 and 21 hr [Color figure can be viewed at wileyonlinelibrary.com]

4 | CONCLUSION

In conclusion, we investigated the effect of replacing the 4T conjugated segment by 3T on the occurrence of polymorphism in PDPP*n*T copolymers. With this structural change, the relative orientation of the DPP units along the main chain likely changes from parallel in PDPP4T to an alternating (right–left) orientation in PDPP3T (Figure 2). The results show that with the proper adjustment of length of the branched alkyl chains on the thiophene rings, to ensure both solubility and aggregation, two different semi-crystalline polymorphs, β_1 and β_2, can be generated in solution and thin films for D-PDPP3T-EH. The β_2 polymorph is more tightly packed along the π–π stacking direction, has a lower optical bandgap, and an increased charge carrier mobility. Although the detailed structural factors that induce polymorphism are still to be described more precisely, we have learned that the oddness or evenness of the number of thiophene rings, does not inhibit generating two distinct semi-

crystalline polymorphs. In fact, for D-PDPP3T-EH, more common solvents such as CB and DCB can form the β_2 polymorph than for PDPP4T polymers. As a common characteristic, we find that the lamellar stacking distance (d_{lam}) of the PDPP*n*T polymers that give a clear $\beta_1 \rightarrow \alpha \rightarrow \beta_2$ polymorphic transition in solution, is between 2.1 and 2.3 nm. When this distance becomes shorter the polymer is strongly aggregating and when it is longer, it is too soluble to provide the necessary balance for the transition to occur.

ACKNOWLEDGMENTS

This work is supported by the National Key R&D Program of China (Grant No. 2019YFA0706100) and the National Natural Science Foundation of China (Grant No. 62074163). We further acknowledge funding from the Netherlands Organization for Scientific Research (016.Veni.192.106 and the NWO Spinoza prize) and the Ministry of Education, Culture and Science (Gravity program 024.001.035).

ORCID

Mengmeng Li https://orcid.org/0000-0003-1117-8106
René A. J. Janssen https://orcid.org/0000-0002-1920-5124

REFERENCES

[1] D. Venkateshvaran, M. Nikolka, A. Sadhanala, V. Lemaur, M. Zelazny, M. Kepa, M. Hurhangee, A. J. Kronemeijer, V. Pecunia, I. Nasrallah, I. Romanov, K. Broch, I. McCulloch, D. Emin, Y. Olivier, J. Cornil, D. Beljonne, H. Sirringhaus, *Nature* **2014**, *515*, 384.
[2] J. Y. Oh, S. Rondeau-Gagné, Y.-C. Chiu, A. Chortos, F. Lissel, G.-J. N. Wang, B. C. Schroeder, T. Kurosawa, J. Lopez, T. Katsumata, J. Xu, C. Zhu, X. Gu, W.-G. Bae, Y. Kim, L. Jin, J. W. Chung, J. B. H. Tok, Z. Bao, *Nature* **2016**, *539*, 411.
[3] M. Li, C. An, W. Pisula, K. Müllen, *Acc. Chem. Res.* **2018**, *51*, 1196.
[4] T. Marszalek, M. Li, W. Pisula, *Chem. Commun.* **2016**, *52*, 10938.
[5] M. Li, D. K. Mangalore, J. Zhao, J. H. Carpenter, H. Yan, H. Ade, H. Yan, K. Müllen, P. W. M. Blom, W. Pisula, D. M. de Leeuw, K. Asadi, *Nat. Commun.* **2018**, *9*, 451.
[6] R. Noriega, J. Rivnay, K. Vandewal, F. P. V. Koch, N. Stingelin, P. Smith, M. F. Toney, A. Salleo, *Nat. Mater.* **2013**, *12*, 1038.
[7] A. Köhler, S. T. Hoffmann, H. Bässler, *J. Am. Chem. Soc.* **2012**, *134*, 11594.
[8] B. M. W. Langeveld-Voss, M. P. T. Christiaans, R. A. J. Janssen, E. W. Meijer, *Macromolecules* **1998**, *31*, 6702.
[9] C. Hellmann, F. Paquin, N. D. Treat, A. Bruno, L. X. Reynolds, S. A. Haque, P. N. Stavrinou, C. Silva, N. Stingelin, *Adv. Mater.* **2013**, *25*, 4906.
[10] G. H. Lu, L. G. Li, X. N. Yang, *Adv. Mater.* **2007**, *19*, 3594.
[11] M. Brinkmann, E. Gonthier, S. Bogen, K. Tremel, S. Ludwigs, M. Hufnagel, M. Sommer, *ACS Nano* **2012**, *6*, 10319.
[12] R. Steyrleuthner, M. Schubert, I. Howard, B. Klaumünzer, K. Schilling, Z. Chen, P. Saalfrank, F. Laquai, A. Facchetti, D. Neher, *J. Am. Chem. Soc.* **2012**, *134*, 18303.
[13] F. S. U. Fischer, D. Trefz, J. Back, N. Kayunkid, B. Tornow, S. Albrecht, K. G. Yager, G. Singh, A. Karim, D. Neher, M. Brinkmann, S. Ludwigs, *Adv. Mater.* **2014**, *27*, 1223.
[14] M. Li, A. H. Balawi, P. J. Leenaers, L. Ning, G. H. L. Heintges, T. Marszalek, W. Pisula, M. M. Wienk, S. C. J. Meskers, Y. Yi, F. Laquai, R. A. J. Janssen, *Nat. Commun.* **2019**, *10*, 2867.
[15] M. Li, P. J. Leenaers, M. M. Wienk, R. A. J. Janssen, *J. Mater. Chem. C* **2020**, *8*, 5856.
[16] S. Qu, H. Tian, *Chem. Commun.* **2012**, *48*, 3039.
[17] C. B. Nielsen, M. Turbiez, I. McCulloch, *Adv. Mater.* **2013**, *25*, 1859.
[18] M. A. Naik, S. Patil, *Polym. Chem.* **2013**, *51*, 4241.
[19] Y. Li, P. Sonar, L. Murphy, W. Hong, *Energy Environ. Sci.* **2013**, *6*, 1684.
[20] Z. Yi, S. Wang, Y. Liu, *Adv. Mater.* **2015**, *27*, 3589.
[21] M. Grzybowski, D. T. Gryko, *Adv. Opt. Mater.* **2015**, *3*, 280.
[22] W. Li, K. H. Hendriks, M. M. Wienk, R. A. J. Janssen, *Acc. Chem. Res.* **2016**, *49*, 78.
[23] A. Tang, *Adv. Mater.* **2017**, *29*, 1600013.
[24] Q. Liu, S. E. Bottle, P. Sonar, *Adv. Mater.* **2020**, *32*, 1903882.
[25] S. Millefiori, A. Alparone, A. Millefiori, *J. Heterocycl. Chem.* **2000**, *37*, 847.
[26] N. Xue, Y. Wei, G. Zhang, L. Liu, L. Zhang, *Chem., Asian J.* **2019**, *14*, 1050.
[27] D. A. Warr, L. M. A. Perdigão, H. Pinfold, J. Blohm, D. Stringer, A. Leventis, H. Bronstein, A. Troisi, G. Costantini, *Sci. Adv.* **2018**, *4*, eaas9543.
[28] G. H. L. Heintges, P. J. Leenaers, R. A. J. Janssen, *J. Mater. Chem. A* **2017**, *5*, 13748.
[29] V. Coropceanu, J. Cornil, D. A. da Silva Filho, Y. Olivier, R. Silbey, J.-L. Brédas, *Chem. Rev.* **2007**, *107*, 926.

SUPPORTING INFORMATION

Additional supporting information may be found online in the Supporting Information section at the end of this article.

How to cite this article: Li M, Leenaers PJ, Li J, Wienk MM, Janssen RAJ. Polymorphism of a semi-crystalline diketopyrrolopyrrole-terthiophene polymer. *J Polym Sci*. 2021;59:1285–1292. https://doi.org/10.1002/pol.20200673